

Neutron star cooling within the equation of state with induced surface tension

S. Tsiopelas, V. Sagun*

CFisUC, Department of Physics, University of Coimbra, 3004-516 Coimbra, Portugal

We study the thermal evolution of neutron stars described within the equation of state with induced surface tension (IST) that reproduces properties of normal nuclear matter, fulfills the proton flow constraint, provides a high-quality description of hadron multiplicities created during the nuclear-nuclear collision experiments, and is equally compatible with the constraints from astrophysical observations and the GW170817 event. The model features strong direct Urca processes for the stars above $1.91 M_{\odot}$. The IST equation of state shows a very good agreement with the available cooling data, even without introducing nuclear pairing. We also analysed an effect of the singlet proton/neutron and triplet neutron pairing on the cooling of neutron stars of different mass. We demonstrate a full agreement of the predicted cooling curves with the experimental data. Moreover, the IST EoS provides a description of Cas A with both paired and unpaired matter.

Keywords: neutron stars, equation of state, cooling

I. INTRODUCTION

Born out of supernova explosions, neutron stars (NSs) are considered to start their life having very high internal temperatures and cool down through a combination of thermal radiation from their surface and neutrino emission from their interior. From the first day of their lives, when the temperature of their interior has already dropped from $\sim 10^{11}$ K to $\sim 10^{9-10}$ K making it transparent to neutrinos, up until the first million years of their existence, thermal energy is carried away mainly in the form of neutrino radiation. During this time, measurements of surface temperature and luminosity of the stars can provide significant information about the properties of matter in their depth, since the thermal evolution depends on factors such as the internal composition and the thermodynamic properties of matter are defined by the Equation of State (EoS), the chemical abundances of the envelope and the type of pairing between the constituent particles. It is, therefore, necessary for any theoretical calculations aiming to describe the cooling process of NSs to consider the various combinations between those factors. The set of cooling curves extracted from these simulations can then be tested against the observable features of NSs in the X-ray part of the spectrum.

The particle composition of the core of NSs plays a prominent role in their cooling process, since it is the decisive factor of whether the direct Urca (DU) process of neutron β -decay and its inverse process are allowed to occur in the interior of the star. These are the most efficient neutrino-emitting reactions that can happen in hadronic matter and, when permitted, they lead to a rapid cooling of the NS, substantially different from the case they are forbidden [17, 19]. For these reactions to be possible, the Fermi momenta of the participating particles must satisfy the kinematic restriction of triangle inequality. Taking into account charge neutrality and the relation between the Fermi momenta and the number density of each par-

ticle, this constraint leads to the requirement that the proton fraction should be higher than $\sim 11\%$ of the total baryon density [17].

Since the composition ultimately depends on the symmetry energy of nuclear matter, the choice of the EoS strongly affects the calculations regarding the thermal evolution of NSs. In this paper, we will use the EoS formulated within the framework of induced surface tension (IST) with its original purpose being the description of experimental data referring to nuclear and hadron matter. The recent results show it can be equally applied to model the properties of symmetric nuclear matter, analysis of hadron yields created at heavy-ion collision from the AGS to ALICE energies, as well as to describe compact astrophysical objects [22–24, 27]. The IST EoS is, furthermore, free of any restraints on the number of included particle species, which makes it highly appropriate for studying the properties of strongly interacting matter at high densities. A comprehensive analysis of the model can be found in Refs. [13, 22]. For a realistic description of the outer layers of the NS the IST EoS is supplemented by the Haensel-Zdunik (HZ) EoS for the outer crust and the Negele-Vautherin (NV) EoS for the inner crust [11, 15].

An additional important factor worth considering is the superfluidity (superconductivity) of neutrons (protons) in the NS interior, since they are able to alter the thermal evolution of the star [32]. Despite suppressing the rates of neutrino emission from the rest of the processes, pairing between protons or neutrons introduces a new ν_e -emitting mechanism due to the permanent formation and breaking of Cooper pairs, known as PBF [19]. This neutrino emitting process is activated in each baryon species as soon as the temperature reaches the respective critical temperatures $T_{c,n}$, $T_{c,p}$. Nevertheless, the details such as the onset T, the form of the gap parameter and the peak of the PBF emissivity are strongly sensitive to the gap model adopted to describe the matter in this supercritical state. As a result, applying different models on the investigation of NS cooling provides also the possibility of gaining a further insight on the behavior of paired matter.

*Emails: st.tsiop@gmail.com, violetta.sagun@uc.pt

Based on the IST EoS, in this work we study the thermal evolution of NSs, aiming to describe the available cooling data. Investigation is focused on the implications of employing various gap models to describe neutron superfluidity and proton superconductivity. In addition, we examine the effect of envelope composition on the cooling process of compact stars. Modeling the thermal evolution of NSs was performed using the *NSCool* code [17, 18].

The paper is organized as follows: In Sec. II we present a brief description of the EoS model. In Sec. III we discuss the neutrino emission mechanisms taking place in a NS as well as the pairing models used in the simulations. Sec. IV is dedicated to the results of the calculations while Sec. V contains the summary and the conclusions.

II. EQUATION OF STATE

The IST EoS is formulated to include neutrons, protons and electrons. It accounts for strong short range repulsion and relatively weak long-range attraction between nucleons, while electrons are treated as an ideal Fermi gas. The former part of the nucleon-nucleon interaction is modelled with the hard core radius, similarly to the famous Van der Waals EoS. The hard core repulsion of nucleons leads to an appearance of excluded volume. However, contrary to the Van der Waals approximation, the IST EoS instead of the constant excluded volume has a density-dependent one. The key element of the model is the IST coefficient. It accounts not only for the correct values of four virial coefficients of hard spheres, but also extends the causality range of the model to the density range typical for the NSs [22, 27]. Moreover, the long-range attraction and asymmetry between neutrons and protons are accounted via the mean-field potentials, parameters of which were fitted to the properties of matter at saturation density. More detailed information about the model and its application to the NSs can be found in Refs. [22, 23, 27].

We adopt the softer parameterisation of the IST EoS that corresponds to the set B of Ref. [21] (for simplicity we keep referring to this parameterisation of the model as set B). The set B was chosen due to the better agreement with the astrophysical constraints and results coming from the GW170817 [1]. It gives the values of the symmetry energy $E_{sym} = 30.0$ MeV, symmetry energy slope $L = 93.2$ MeV and nuclear incompressibility factor $K_0 = 201.0$ MeV at normal nuclear density that is in full agreement with the present nuclear matter results [22, 23]. As it is shown on Fig.1 the maximum mass $M_{max} = 2.08M_{\odot}$ is consistent with the recent measurements of the most massive NSs, i.e. PSR J0348+0432 [4] and PSR J0740+6620 [9].

III. COOLING PROCESSES

The thermal evolution of NSs can be divided in two stages. During the first one, known as neutrino cooling

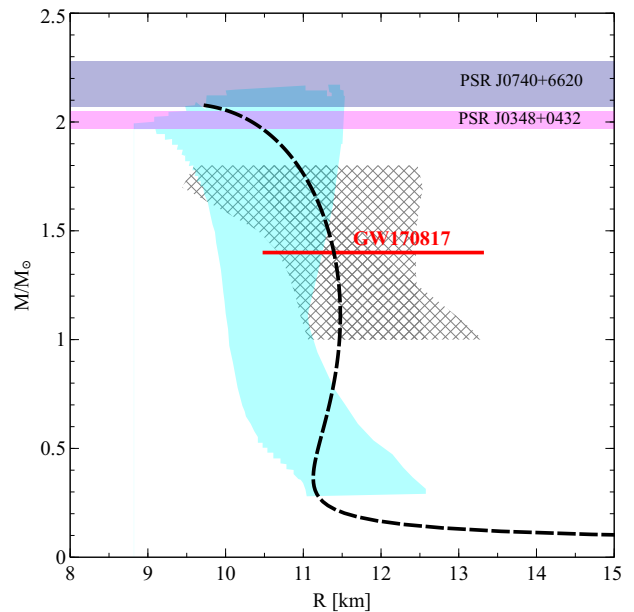


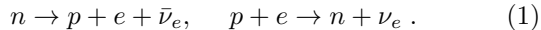
FIG. 1: Mass-radius relation for non-rotating NSs calculated for set B of the IST EoS [21]. Horizontal bands correspond to the two most massive NSs, e.g. PSR J0348+0432 [4] (magenta band) and PSR J0740+6620 [9] (blue band). The shaded grey area represents the M-R constraint taken from Refs. [29, 30], while the constraint depicted as a cyan area was taken from Ref. [16]. The red line represents the allowed range of NS radius, according to GW170817 event.

era, ν_e emission generated from a plethora of emission mechanisms throughout the whole interior of the star dominates the cooling process [17, 19]. On a timescale of a million years after the NS formation, when T_{core} has dropped below 10^8 K, neutrino emission from the core is less efficient due to the strong temperature dependence, and photon emission from the surface overtakes as the leading heat loss mechanism. Beyond this point, the neutrino cooling era is over and the photon cooling era begins. This shift is marked by an abrupt decline of the total luminosity and surface temperature of the star, with more massive stars exhibiting steeper drops of those quantities than less massive ones, since photon luminosity follows the typical blackbody radiation law.

During the neutrino cooling era, the leading neutrino-generating process varies over the regions of the star and over time. Overall, the main factors regulating the neutrino emissivity of each process are density, temperature and the existing degree of Cooper pairing between particles. For example, in the envelope of the star pair annihilation is the most productive mechanism, while in the outer crust neutrino emission is dominated by plasmon decay until its temperature reaches a few times 10^8 K, replaced by electron-ion bremsstrahlung beyond that point [19, 32]. The latter remains the most efficient energy loss mechanism throughout the inner crust as well, as long as the neutrons of this region are paired [14]. Even in their supercritical state though,

inner crust neutrons contribute to the total neutrino emission through the PBF process over a narrow range of densities and temperatures [19].

In the core of the star, apart from the bremsstrahlung processes between the free particles, the main neutrino-emitting processes that can occur are the DU process of the neutron β -decay and its inverse:



As it was mentioned above, the realization of these reactions depends on the proton fraction in the star interior. For the IST EoS adopted in this work, these fast processes can only proceed in the core of stars with central densities n_c higher than $n_{DU} = 0.862 \text{ fm}^{-3}$. For NSs with lower n_c , where the Fermi momenta of the involved particles fail to satisfy the kinematic restriction of $p_{F,n} \leq p_{F,p} + p_{F,e}$, neutron β -decay and its inverse can still proceed with the help of a spectator proton or neutron that provides the extra $p_{F,i}$ needed for the conservation of momentum. In this case, though, the efficiency of these so-called modified Urca (MU) processes in removing heat from the star is lower than that of the DU ones, resulting in an overall slower cooling of the star. Nevertheless, neutrino emission from MU processes surpasses the rest of the emissivities in the core, unless n and p are in a paired state, which in turn results in a further suppression of the neutrino emission rates. However, pairing partially compensates for the delay in the cooling of the NS core as it introduces PBF, an additional efficient channel for carrying the heat away in the form of neutrino-antineutrino pairs [19].

Cooper pairing of core protons and crust neutrons sets in a few years after the NS birth, while core neutrons pairing is viable at a later time. As regards the types of pairing, all of them follow the standard BCS pattern, with free neutrons of the inner crust and protons of the core undergoing singlet-state pairing (1S_0), while neutrons of the core are expected to pair in the triplet-state (3P_2) [5, 6, 17]. Although a complete, precise description of the effect for densities relevant to NS matter is still pending, it is widely applied for investigating its imprint on the thermal evolution of compact stars. The transition of neutrons(protons) to superfluid(superconducting) state inflicts a suppression on their specific heat as well. Most studies agree that once it switches on for a certain species, $c_{v,i}$ is reduced by a factor $\mathcal{R} \sim e^{-\Delta/T}$, where Δ is the gap parameter, linked to the respective critical temperature T_c via the standard BCS pairing relation $T_c \approx 0.57\Delta$ [5, 6, 17]. A further drop in temperature, causes a further reduction of heat capacity to the point of being equal to that of leptons [19]. Concerning the neutrino emissivity of processes involving paired baryons, suppression is induced as well, since particles in such a supercritical state have to overcome the energy gap, in order to interact with another particle. In the range of temperatures $T \ll T_c$, this behavior is illustrated numerically using a yet another set of control functions $\mathcal{R}_\chi(T/T_c)$, which differs between each particle

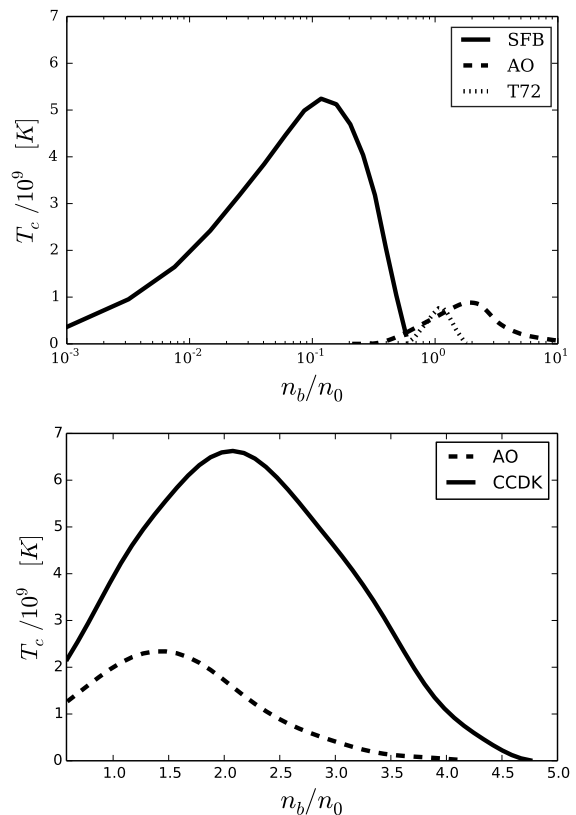


FIG. 2: Density dependence of the critical temperature for the considered singlet and triplet neutron gaps (upper panel) and proton singlet pairing gaps (lower panel).

species χ [32].

The onset temperatures $T_{c,n}(T_{c,p})$ of superfluidity (superconductivity), the associated Δ and the profile of PBF neutrino emissivity vary over the several models developed to describe the paired matter. Therefore, when including nucleon pairing for simulating the thermal evolution of NSs, the effect is subject to the gap models employed. Our choice for the simulations were the following models: SFB [28] for the 1S_0 superfluidity of neutrons, T72 [31] and AO [2] for their 3P_2 superfluidity, and AO [3], CCDK [8] for the proton 1S_0 channel in different combinations. The critical temperatures T_c were calculated according to the phenomenological formula suggested by Kaminker et al. and the parameters used by Ho et al. [12, 14].

The relation between the critical temperature and the baryon density for all the adopted gap models is shown on Fig.2. According to the SFB model, 1S_0 pairing of crust neutrons appears first at densities around $0.15 n_0$, once the crust temperature has dropped below $\sim 5 \cdot 10^9 \text{ K}$. As the crust keeps cooling, the region of superfluid crust neutrons expands both outwards and towards the crust-core interface. Regarding superconductivity of protons in the core, CCDK model suggests that the proton pairing occurs initially at a temperature not greater than $7 \cdot 10^9 \text{ K}$ in the layer corresponding to $\sim 2 n_0$. On the

contrary, AO model proposes that the onset temperature is a few times lower, at $2 \cdot 10^9 K$, while the associated baryon density only slightly lower. Finally, as claimed by the T72 model, the threshold for the onset of 3P_2 superfluidity of core neutrons is below $10^9 K$ and pairing occurs in a narrow, symmetric region centered around the normal nuclear density n_0 . The respective AO model, on the other hand, although it does not differ considerably in terms of $T_{c,n}$, implies that neutron pairing can occur throughout the whole region of the core.

The composition of the envelope is another deciding factor for the surface photon luminosity of the star, which is ultimately the quantity of observational importance. Namely, heavier elements tend to delay heat transport from the outer crust to the surface, since in this case the electron thermal conductivity is reduced [33]. The standard approach of thermal evolution codes is to set an envelope model as an outer boundary condition that links the temperature at the bottom of the envelope (T_b) to the temperature of the stellar surface (T_s). The fundamental assumptions behind this method are that the envelope has a thermal relaxation timescale which is much shorter than that of the crust, and that the neutrino emissivity in the envelope is negligible [17]. In this work, we used two distinct envelope models: one composed of heavy elements (Fe) and a hydrogen-rich one that contains the fraction of light elements $\eta = \Delta M/M = 10^{-7}$ [20].

IV. RESULTS

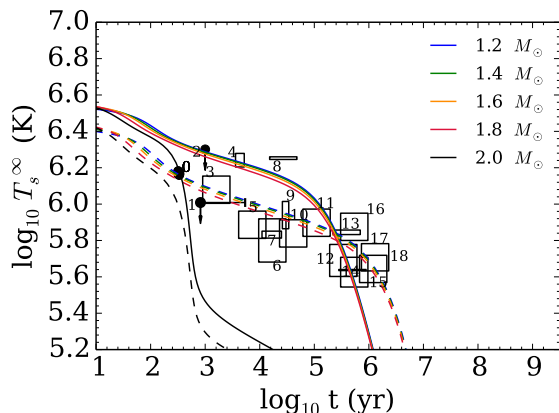


FIG. 3: Cooling curves for stars of different mass $M/M_\odot = 1.2, 1.4, 1.6, 1.8, 2.0$ for the case of unpaired matter. T_s^∞ denotes the surface temperature at infinity. The solid curves correspond to the light-element envelope ($\eta = 10^{-7}$), while the dashed curves were obtained for the Fe envelope. The data points are taken from [7].

At the beginning we focused on the thermal evolution of NSs without any sort of pairing between the nucleons. As you can see on Fig.3 all the cooling curves depicted in color exhibit a slow cooling due to the domination of the MU processes, since the DU ones are

not kinematically allowed. Finally, at central densities of over $n_{DU} = 0.862 fm^{-3}$ of beta-stable and charge neutral matter, which correspond to NSs with masses $M \geq 1.91 M_\odot$, the DU processes are switched on in the core of the star so that it undergoes enhanced cooling (see the black curves on Fig.2). In order to model the uncertainties of the heat-blanketing effect of the envelope, we compare the thermal evolution of NSs with a non-accreted envelope containing heavy elements (dashed curves on Fig.3) with the envelope containing light elements (solid curves on Fig.3).

Remarkably, the obtained cooling curves for unpaired matter describe the experimental data very good. In addition, we would like to stress the description of the NS in the Cassiopeia A (Cas A) supernova remnant, that corresponds to the star noted as 0 on Fig.2. Namely, we find that Cas A can be equally described by both a rapidly cooling $2 M_\odot$ star with a light-elements envelope and a slow cooling low-mass star with a Fe envelope.

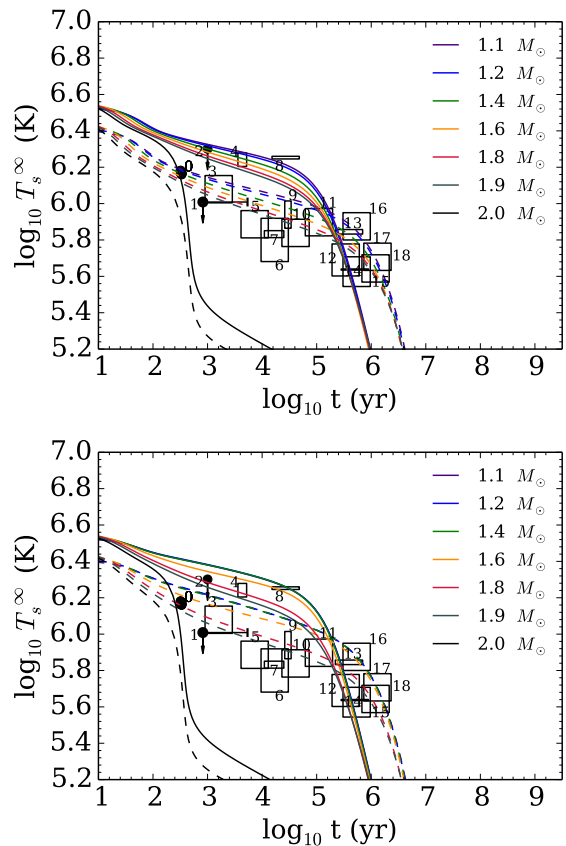


FIG. 4: The same as Figure 3, but considering the effect of neutron superfluidity in the 1S_0 channel via the SFB model [28] and proton superconductivity in the 1S_0 channel with the AO model [2] (upper panel) and CCDK model [8] (lower panel).

This result thus leaves an equal possibility for both cooling scenarios. As a matter of fact, Cas A is a highly debatable object; as was discussed in many papers including Refs.[34-37], some data of Cas A indicate a rapid

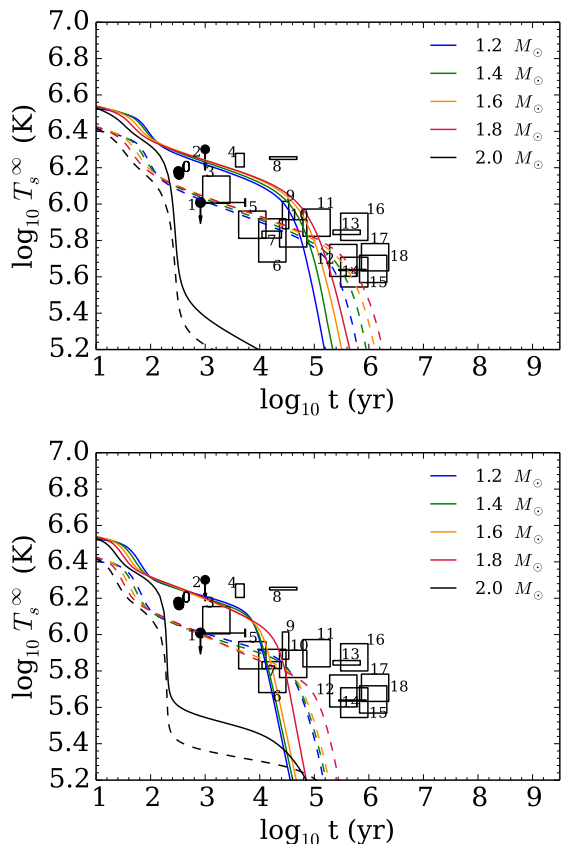


FIG. 5: The same as lower panel of Figure 4, but supplemented with the triplet neutron pairing in the core of the star described by the T72 model [31] (upper panel) and the AO model [3] (lower panel).

cooling with a few percent drop of the surface temperature across 10 years of observations, while other data suggest a slower cooling.

Furthermore, we studied the effect of neutron superfluidity and proton superconductivity on the thermal evolution of NSs in two stages. First, we considered n^1S_0 superfluidity with the SFB model [28] together with a p^1S_0 superconductivity described by AO [3] and CCDK [8] models (see Fig.4). For both considered combinations of gaps, i.e. SFB+AO (see the upper panel on Fig.4) and SFB+CCDK (see the lower panel on Fig.4), the IST EoS is in very good agreement with the experimental data. As in the non-superfluid case, the model predicts the surface temperature for the Cas A both with the fast cooling curve for $M_{DU} = 2.0 M_\odot$, as well as with the curves for low-mass stars with a heavy-elements envelope. For the SFB+CCDK gaps the Cas A is only described with a curve for $M = 1.8 M_\odot$ also with an Fe envelope.

Finally, we studied the effect of the neutron triplet pairing on the cooling of NSs by considering a shallow

gap with a maximum of the critical temperature at the saturation density n_0 (T72 model [31]) and an extended gap with a maximum of T_c at $2n_0$ (AO model [3]). As it is shown on Fig.5 the combination of models SFB(for n^1S_0)+T72(for n^3P_2)+CCDK (for p^1S_0) (upper panel) and SFB(for n^1S_0)+AO(for n^3P_2)+CCDK (for p^1S_0) (lower panel) give qualitatively similar result. Adding the n^3P_2 pairing in the core of NSs leads to more rapid cooling and makes it incompatible with most of the observational data. Therefore, we conclude that within our model, neutron pairing in the triplet channel is inconsistent with the experimental data.

V. CONCLUSIONS

We studied the cooling of NSs with the novel IST EoS that was previously applied to the analysis of nuclear matter properties, heavy-ion collision experimental data, and was recently generalized for the description of matter inside NSs. The considered model parameterisation is in good agreement with the GW170817 and the recent measurements of the most massive NSs. For the stars with $M \geq 1.91 M_\odot$ the model allows for the occurrence of DU processes that leads to much faster cooling. An effect of neutron pairing in 1S_0 and 3P_2 channels, as well as proton pairing in 1S_0 channel is thoroughly analysed with different superfluidity/superconductivity models. In addition, effects of different types of envelopes on the thermal evolution of NSs were also compared. We show that for unpaired matter the obtained cooling curves are fully consistent with the currently existing observational data. Remarkably, the IST EoS with unpaired matter predicts the surface temperature of Cas A both with the fast cooling curve for $M_{DU} = 2.0 M_\odot$ with the accreted envelope of light-elements and the low-mass star with the heavy-elements envelope.

The presence of the proton(neutron) superconductivity(superfluidity) in the singlet channel slightly slows down the cooling and makes the agreement with the data even better. The two considered scenarios of the triplet neutron pairing in the core of the star (a shallow and an extended neutron superfluidity) lead to too rapid cooling of all NSs, such that the old stars ($t > 10^5$ yr) cannot be reproduced. Thus, we can conclude that the calculations favours the vanishing neutron triplet pairing gap.

VI. ACKNOWLEDGEMENTS

We are thankful for the fruitful discussions and suggestions to M. Fortin and O. Ivanytskyi. V.S. acknowledges the support from the Fundação para a Ciência e Tecnologia (FCT) within the project UID/04564/2020.

[1] B.P. Abbott et al. (LIGO and Virgo Collab.), Phys. Rev. Lett. 119, 161101 (2017).

[2] L. Amundsen, E. Ostgaard, Nucl. Phys. A, **437**, 487

- (1985a).
- [3] L. Amundsen, E. Ostgaard, Nucl. Phys. A, **442**, 163 (1985b).
- [4] J. Antoniadis, P. C. C., Freire, N. Wex *et al.*, Science, **340**, 6131, 448 (2013).
- [5] J. Bardeen, L. N. Cooper and J. R. Schrieffer, Phys. Rev., **108**, 1175 (1957).
- [6] W. Becker, Neutron Stars and Pulsars, Springer (2009).
- [7] M. V. Beznogov, D. G. Yakovlev, Mon. Not. R. Astron. Soc., **447**, 2, 1598, 2015.
- [8] J. M. C. Chen, J. W. Clark *et al.*, Nuclear Physics A, **555** 59 (1993)
- [9] H. T. Cromartie, E. Fonseca, S. M. Ransom *et al.*, Nature Astr., **4**, 72 (2020).
- [10] P. B., Demorest, T. Pennucci, S. M. Ransom *et al.*, Nature, **467**, 7319, 1081 (2010).
- [11] P. Haensel, J. L. Zdunik, A& A, **229**, 117 (1990).
- [12] W. C. G. Ho, K. G. Elshamouty, C. O. Heinke, A. Y. Potekhin, Phys. Rev. C, **91**, 015806 (2015)
- [13] A. I. Ivanytskyi, K. A. Bugaev, V. V. Sagun, L. V. Bravina, E. E. Zabrodin, Phys. Rev. C, **97**, 064905 (2018).
- [14] A. D Kaminker, P. Haensel and D. G. Yakovlev, A& A, **373** 2 (2001).
- [15] J. W. Negele, D. Vautherin, Nucl. Phys. A, **207**, 298 (1973).
- [16] F. Özel, P. Freire, An. Rev. Astr. & Astroph., **54**, 401 (2016).
- [17] D. Page, U. Geppert, F. Weber, Nucl. Phys. A, **777**, 497 (2006).
- [18] D. Page, S. Reddy, Annu. Rev. Nucl. & Part. Sci., **56**, 327 (2006).
- [19] A. Y. Potekhin, J. A. Pons, D. Page, Sp. Sci. Rev., **191**, 239 (2015).
- [20] A. Y. Potekhin, D. G. Yakovlev, G. Chabrier, O. Y. Gnedin, Astrophys. J. **594**, 1, 404 (2003).
- [21] V. Sagun, G. Panotopoulos, I. Lopes, Phys. Rev. D, **101**, 063025 (2020).
- [22] V. V. Sagun, I. Lopes, A. I. Ivanytskyi, Astrophys. J. **871**, 157 (2019).
- [23] V. Sagun, I. Lopes, A. Ivanytskyi, Nucl. Phys. A, **982**, 883 (2019).
- [24] V. V. Sagun, K. A. Bugaev, A. I. Ivanytskyi, I. P. Yaki-menko *et al.*, Eur. Phys. J. A, **54**, 6, 100 (2018).
- [25] V. V. Sagun, K. A. Bugaiev, A. I. Ivanytskyi, D. R. Oli-inychenko *et al.*, Eur. Phys. J. Web Conf. **137**, 09007 (2017).
- [26] V. V. Sagun, I. Lopes, Astrophys. J. **850**, 1, 75 (2017).
- [27] V. V. Sagun, A. I. Ivanytskyi, K. A. Bugaev, I. N. Mishustin, Nucl. Phys. A, **924**, 24 (2014).
- [28] A. Schwenk, B. Friman, G. E. Brown, Nucl. Phys. A, **713**, 191 (2003).
- [29] A. W. Steiner, J. M. Lattimer, E. F. Brown, Astrophys. J., **722**, 1, 33 (2010).
- [30] A. W. Steiner, J. M. Lattimer, E. F. Brown, Astrophys. J., **765**, L5 (2013).
- [31] T. Takatsuka, Prog. Theor. Phys., **48**, 1517 (1972).
- [32] D. G. Yakovlev, A. D. Kaminker, O. Y. Gnedin, P. Haensel, Phys. Rep., **354**, 1 (2001).
- [33] D. G. Yakovlev, V. A. Urpin, Soviet Astronomy, **24**, 303 (1980).
- [34] W. C. G. Ho, O. C. Heinke, Nature, **462**, 7269, 71 (2009)
- [35] O. C. Heinke, W. C. G. Ho, Astrophys. Journal Lett., **719**, 2, L167 (2010)
- [36] B. Posselt, G. G. Pavlov, Astrophys. J., **864**, 2, 7 (2018)
- [37] G. Taranto, F. G. Burgio, H.-J. Schulze, Mon. Not. R. Astron. Soc., **456**, 2, 1451 (2016)